


Band engineering in an epitaxial two-dimensional honeycomb Si_{6-x}Ge_x alloyA. Fleurence^{1,*}, Y. Awatani,¹ C. Huet,¹ F. B. Wiggers^{2,†}, S. M. Wallace,¹ T. Yonezawa,¹ and Y. Yamada-Takamura¹¹*School of Materials Science, Japan Advanced Institute of Science and Technology, 1-1 Asahidai Ishikawa 923-1292, Japan*²*MESA+ Institute for Nanotechnology, University of Twente, 7500 AE Enschede, The Netherlands* (Received 26 February 2020; revised 16 October 2020; accepted 8 December 2020; published 21 January 2021)

In this Letter, we demonstrate that it is possible to form a two-dimensional (2D) silicene-like Si₅Ge compound by replacing the Si atoms occupying on-top sites in the planar-like structure of epitaxial silicene on ZrB₂(0001) by deposited Ge atoms. For coverages below 1/6 monolayer, the Ge deposition gives rise to a Si_{6-x}Ge_x alloy (with x between 0 and 1) in which the on-top sites are randomly occupied by Si or Ge atoms. The progressive increase of the valence band maximum with x observed experimentally originates from a selective charge transfer from Ge atoms to Si atoms. These achievements provide evidence for the possibility of engineering the band structure in 2D SiGe alloys in a way that is similar for their bulk counterpart.

DOI: [10.1103/PhysRevMaterials.5.L011001](https://doi.org/10.1103/PhysRevMaterials.5.L011001)

Alloying materials with similar structures and miscible elements is of great interest for a wide range of applications as it allows for adjusting various parameters to values which cannot be achieved with elemental materials or compounds. This versatility is well exemplified by the engineering of the band gap of semiconducting alloys which makes possible the fine-tuning of the wavelength of solid-state lightings by controlling the alloys composition. With the continuous efforts to scale down the dimension of elementary bricks of electronic devices, the fabrication of low-dimensional alloys, including two-dimensional (2D) materials, became a technologically important challenge [1] as it was for bulk semiconducting materials in the past. Alloying semimetallic graphene, with its isomorphous wide-band-gap analog h-BN, which would have permitted one to set the value of the band gap of a 2D h-BNC alloy in a wide energy range, was, however, found to be hindered by the low miscibility of the two materials resulting in a phase segregation [2]. In contrast, ternary and quaternary alloys of transition metal dichalcogenide could be synthesized successfully [3–7] and the tunability of the optical band gap was demonstrated. Among the 2D materials experimentally fabricated, silicene, a 2D honeycomb lattice made of Si atoms, has the particularity to allow for continuing scaling down of the Si-based nanoelectronics [8]. Freestanding silicene is predicted to possess Dirac cones in its band structure [9,10]. However, the flexibility of silicene atomic structure and the interaction with the substrate could result in very different band structures for epitaxial forms of silicene [11–14]. Thorough efforts were put into evaluat-

ing methods for tuning the electronic properties of silicene including doping [15,16], or the adsorption of adatoms or molecules [17–19]. Alloying freestanding forms of silicene and germanene, its Ge analog, investigated by first-principles calculations [20–22] suggested that such 2D hexagonal SiGe alloys are stable and various parameters including the lattice parameter or the spin-orbit gap opening in the Dirac cones were found to be tunable with the Si:Ge ratio while the non-triviality of the band structure is preserved.

In this Letter, we report the realization of a 2D SiGe epitaxial alloy fabricated by depositing Ge on silicene on zirconium diboride (ZrB₂) films grown on Si(111) [23]. Furthermore, we investigated the possibility of engineering its band gap in a way similar to bulk SiGe alloys.

Epitaxial silicene sheets were prepared by annealing ZrB₂ thin films epitaxially grown on Si(111) [24,25] in ultrahigh vacuum (UHV). The deposition of Ge on silicene was realized by means of a Knudsen cell implemented in each of the UHV systems used for these experiments. The Ge flux was calibrated in each of these systems by depositing Ge on Si(111) and by recording surface-sensitive Auger electron and/or core-level photoelectron spectra. The evolution of the intensity of Ge and Si peaks during the deposition of Ge on Si(111) with the deposition time show changes in the slope which correspond to coverages of 1 and 2 Ge monolayers. Scanning tunneling microscopy (STM) was used to verify the formation of Ge huts on Si(001) at the expected coverage threshold. The fluxes were estimated to be $0.09 \pm 0.01 \text{ ML min}^{-1}$ for the setup used for photoemission experiments and $0.11 \pm 0.01 \text{ ML min}^{-1}$ for that used for STM [1 monolayer (ML) refers to the density of atoms in epitaxial silicene on ZrB₂(0001): $1.73 \times 10^{15} \text{ at. cm}^{-2}$]. The coverage is defined as being the flux multiplied by the deposition time. All Ge depositions were done at 350 °C. STM was performed at room temperature. Photoelectron spectroscopy experiments were conducted at beamline BL6U of UVSOR-III synchrotron at the Institute for Molecular Science (IMS). Core-level spectra in normal emission and angle-resolved photoemission spectroscopy (ARPES) spectra were recorded

*antoine@jaist.ac.jp

†Present address: ASML Netherlands B.V., De Run 6501, 5504 DR Veldhoven, The Netherlands.

Published by the American Physical Society under the terms of the [Creative Commons Attribution 4.0 International license](https://creativecommons.org/licenses/by/4.0/). Further distribution of this work must maintain attribution to the author(s) and the published article's title, journal citation, and DOI.

at room temperature and at 20 K, respectively. The respective energy resolutions as estimated from the broadening of the Fermi edge are 35 and 10 meV.

Density functional theory (DFT) calculations within the generalized gradient approximation developed by Perdew, Burke, and Ernzerhof [26,27] were performed using the OPENMX code [28] based on norm-conserving pseudopotentials generated with multireference energies [27] and optimized pseudoatomic basis functions [28]. Input structures consist of (2×2) $\text{ZrB}_2(0001)$ slabs made of eight Zr and seven B layers terminated on both faces, respectively, by silicene or Si_5Ge layers. A 42 \AA vacuum space is separating the slabs. For Zr atoms, an $s3p2d2$ basis function, i.e., including three, two, and two optimized radial functions allocated, respectively, to the s , p , and d orbitals. For Si, Ge, and B atoms, $s2p2d1$ basis functions were adopted. A cutoff radius of 7 bohrs was chosen for all the basis functions. A regular mesh of 220 Ry in real space was employed for the numerical integrations and for the solution of the Poisson equation. A $(5 \times 5 \times 1)$ mesh of k points was used. For geometrical optimization, the force on each atom was relaxed to be less than 0.0001 hartree/bohr. In order to take into account the strength of translational symmetry breaking, the spectral weight as derived from the imaginary part of the one-particle Kohn-Sham Green's function, was unfolded to the Brillouin zone of the "one-Si-atom unit cell" [11] following a method described in Ref. [29]. (4×4) $\text{ZrB}_2(0001)$ slabs terminated on both sides by $\text{Si}_{0.75}\text{Ge}_{0.25}$ structures were used to simulate STM images.

Silicene crystallizes spontaneously on $\text{ZrB}_2(0001)$ thin film surface in a so-called "planarlike" ($\sqrt{3} \times \sqrt{3}$)-reconstructed structure [11,30] adopted by several forms of epitaxial silicene [31–33]. This structure fits with the (2×2) unit cell of $\text{ZrB}_2(0001)$ in such a way that $a_{\text{Si}} = \frac{2}{\sqrt{3}} a_{\text{ZrB}_2}$, where a_{ZrB_2} (3.178 Å) and a_{Si} (3.65 Å) are the lattice parameters of unreconstructed $\text{ZrB}_2(0001)$ and silicene, respectively. Figures 1(a) and 1(b) show the details of the planarlike structure as the result of optimization in DFT calculations. In this structure, two, three, and one Si atoms are respectively sitting on hollow, bridge, and on-top sites of the Zr-terminated thin films. All of the Si atoms but one are laying 2.3 Å above the topmost Zr layer, whereas the Si atoms sitting on the on-top sites visible in STM images are protruding at 3.9 Å. As shown in the STM image of Fig. 1(c), the deposition of 0.05 ML Ge on silicene turns the domain structure of the pristine silicene sheet [24,34] into a single domain in a way similar to the deposition of silicon [35]. However, in contrast to silicon atoms, the deposition of Ge atoms results in a contrast between the protrusions, observed for all scanning conditions, and most visible for a sample bias voltage of 1.0 V. In this condition, the difference of apparent height is $0.18 \pm 0.02 \text{ \AA}$. The suggested substitution of some protruding Si atoms by Ge atoms is confirmed by the fact that the number of tall protrusions (32.1%) in Fig. 1(c) is very close to the number expected for the complete integration of Ge atoms in on-top sites (33.3%) of the silicene structure, which in turn indicates that Ge atoms only replace Si atoms occupying protruding sites. One can also deduce that the sticking coefficient of the Ge adatoms is very close to unity. As this Ge coverage is beyond that required to fully turn the domain structure of silicene into a single domain (0.03

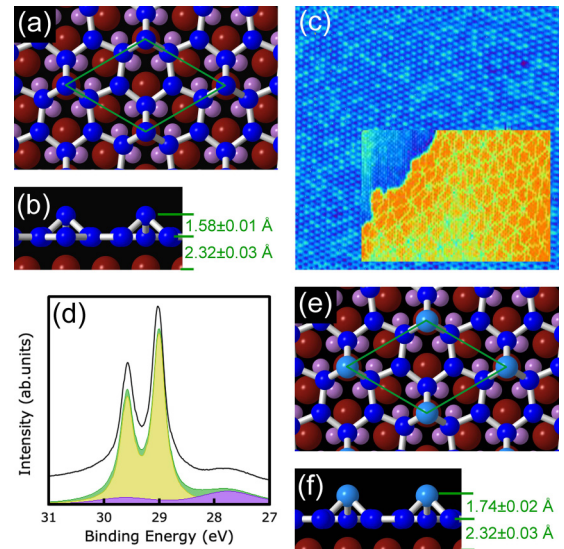


FIG. 1. Deposition of Ge on silicene on $\text{ZrB}_2(0001)$. (a) and (b) Top and side views of the epitaxial planarlike structure of silicene on $\text{ZrB}_2(0001)$ as determined by DFT calculations. Si, Zr, and B atoms are, respectively, dark-blue, red, and purple colored. The green rhombus indicates the $(\sqrt{3} \times \sqrt{3})$ -reconstructed unit cell. (c) STM image ($30 \text{ nm} \times 30 \text{ nm}$, $V = 1.0 \text{ V}$, $I = 100 \text{ pA}$) of epitaxial silicene after deposition of 0.057 ML Ge. The STM image ($33 \text{ nm} \times 23 \text{ nm}$) in the inset shows the silicene-Ge alloy (top left) and Si bilayer islands side-by-side. (d) Photoelectron spectrum recorded with $h\nu = 80 \text{ eV}$ in the Ge $3d$ and Zr $4p$ regions after deposition of 0.090 ML Ge. The experimental spectrum is indicated by the black line. Yellow- and purple-filled curves are the contribution of Ge $3d$ and Zr $4p$ core levels determined by fitting and the green-filled curve is their sum. The full widths at half maximum are 270 and 290 meV, respectively, for the Ge $3d_{3/2}$ and Ge $3d_{5/2}$ peaks. (e) and (f) Top and side views of the structure of epitaxial Si_5Ge on $\text{ZrB}_2(0001)$ as determined by DFT calculations. Si, Zr, and B atoms are colored in the same way as in (a) and Ge atoms are light-blue colored.

ML) [35], the excess of atoms results locally in the formation of bilayer silicon islands [36] like the one shown in the inset of Fig. 1(c). These islands are rare and distant (a few hundreds of nanometers from each other).

Figure 1(d) shows a photoelectron spectrum recorded with a photon energy of $h\nu = 80 \text{ eV}$ in the region of the Zr $4p$ and Ge $3d$ core levels after deposition of 0.09 ML Ge. The fact that the Ge $3d$ component can be fitted with a single pair of Lorentzian functions, points out that the Ge atoms are incorporated into a single site, i.e., the on-top sites of the silicene lattice. It also confirms the STM observation that the formation of Ge islands on the surface is negligible.

Planarlike structures in which a Si atom per silicene- $(\sqrt{3} \times \sqrt{3})$ unit cell was substituted by a Ge atom were investigated by DFT (Fig. 1 of the Supplemental Material [37]). The comparison of the energy of the geometrically optimized structures shows that, in agreement with the experimental observation, the most stable position is the protruding on-top site. Figure 1(d) presents such a planarlike structure, which appears to be essentially similar to that shown in Fig. 1(a). The main difference is the length of the bonds between atoms of the on-top and bridge sites which increases from 2.37 to 2.47 Å. This distance is longer than that of the Si-Ge

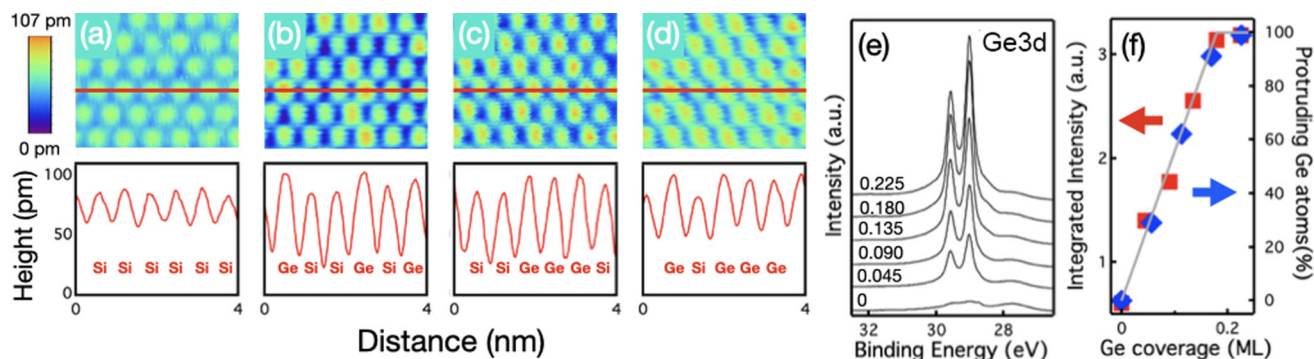


FIG. 2. $\text{Si}_{6-x}\text{Ge}_x$ alloy. (a)–(d) STM images ($V = 1.0$ V, $I = 100$ pA) and profiles along the red lines after deposition of (a) 0.030 ML Si and (b)–(d) 0.057, 0.113, and 0.167 ML Ge. Their common color-coded z scale bar is shown. (e) Spectra recorded in the Ge $3d$ and Zr $4p$ core-level regions recorded for different Ge coverages with a photon energy of 80 eV. (f) Integrated intensity of the photoelectron spectra and percentage of protruding Ge atoms as functions of the Ge coverage.

bonds measured in bulk SiGe alloys [38] or calculated for 2D hexagonal SiGe alloys [21]. The Ge atom is located 1.74 Å above the bottom Si atoms instead of 1.58 Å for the on-top Si atom in silicene, which is in agreement with the fact that these protrusions appear taller for all bias voltage tried for scanning the 2D SiGe alloy. The comparison of simulated STM images (Fig. 2 of the Supplemental Material [37]) confirms that the contrast between protrusions can only be explained by the substitution of Si atoms occupying the on-top sites by Ge atoms. Figure 2 shows the evolution with the Ge coverage of the silicene sheet as imaged by STM and photoelectron spectra recorded in the Zr $4p$ and Ge $3d$ core-level regions. The number of protruding Ge atoms and the integrated intensity of the spectrum increase both linearly until a Ge coverage of 0.17 ML close to the density of protruding atoms in the planarlike structure (1/6 ML) is reached. The fact that at this coverage, all protruding sites are occupied by Ge atoms, demonstrates further that below this coverage, Ge adatoms are fully incorporated into the silicene sheet and replace systematically protruding Si atoms in the planarlike structure. This shows that it is possible to fabricate a 2D $\text{Si}_{6-x}\text{Ge}_x$ alloy with x being

finely adjustable between 0 and 1 by depositing a controlled amount of Ge in this coverage range. As x can be determined with the Ge coverage, the STM images of Figs. 2(a)–2(d) show $\text{Si}_{6-x}\text{Ge}_x$ alloys with x being estimated to be 0, 0.33, 0.66, and 0.98, respectively. The saturation of the intensity of the Ge $3d$ peaks slightly above $x = 1$ can be explained by the surface sensitivity of the radiation and by the formation of Ge islands on top of the SiGe alloy. The extinction of the contribution of the Ge atoms within the alloy covered by islands is compensated by the contribution of Ge atoms in the islands.

To determine the effect of the Ge atoms on the band structure of $\text{Si}_{6-x}\text{Ge}_x$, ARPES spectra were recorded for different values of x between 0 and 1. Figure 3 shows spectra recorded with a photon energy of 45 eV in the region of the K point of the Brillouin zone of unreconstructed silicene where the valence band maximum (VBM) is located [11,24,30]. One can see that the top of the binding energy of the valence band E_{VBM} evolves steadily from $E_{VBM}^{\text{silicene}} = 0.42$ eV for silicene to $E_{VBM}^{\text{Si}_5\text{Ge}} = 0.28$ eV for Si_5Ge , whereas the bottom of the band remains at a binding energy of 1.0 eV. The evolution of E_{VBM} with x is not linear and the fitting of $\Delta E_{VBM} =$

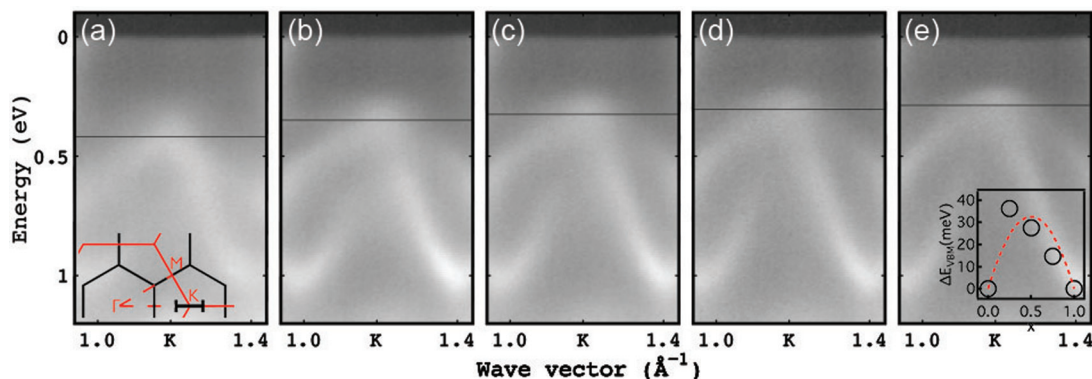


FIG. 3. Valence band of $\text{Si}_{6-x}\text{Ge}_x$ alloy. The inset of (a) shows the region around the K point of the Brillouin zone of unreconstructed silicene in which the spectra were recorded. Brillouin zones of $(\sqrt{3} \times \sqrt{3})$ -reconstructed and unreconstructed silicene are respectively indicated by black and red lines. (a)–(e) ARPES spectra recorded with a photon energy of $h\nu = 45$ eV on $\text{Si}_{6-x}\text{Ge}_x$ alloys for $x = 0, 0.25, 0.5, 0.75,$ and 1. The horizontal lines indicate E_{VBM} . The inset of (e) shows $\Delta E_{VBM} = E_{VBM} - [E_{VBM}^{\text{silicene}}x + E_{VBM}^{\text{Si}_5\text{Ge}}(1-x)]$ as a function of x . Its fitting with $b x(1-x)$ and $b = -125$ meV is indicated by a dashed red line.

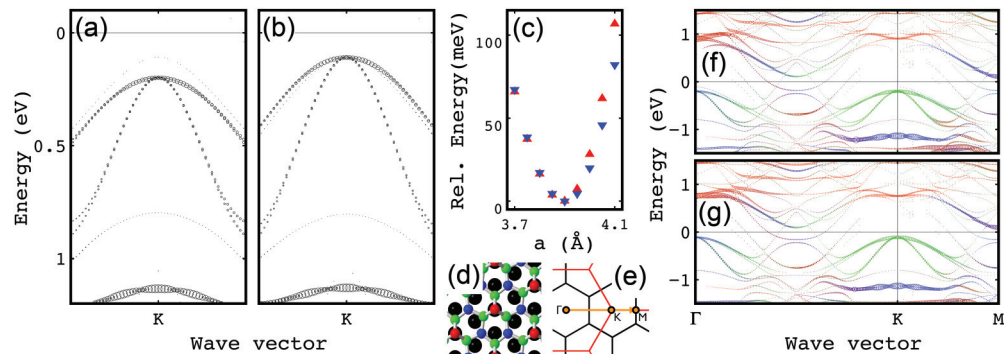


FIG. 4. Calculated band structures of silicene and Si_5Ge . (a) and (b) Band structures of silicene and Si_5Ge in the region indicated in the inset of Fig. 3(a). The spectral weight of the combined contribution of Si and Ge atoms is indicated by the size of the circles. (c) Lattice parameter dependence of the energy per atom of freestanding planarlike structures of silicene (red) and Si_5Ge (blue). (d) Schematics of the planarlike structure on Zr-terminated $\text{ZrB}_2(0001)$. Zr, on-top, bridge, and hollow atoms are respectively black, red, green, and blue colored. (e) Schematics of the k space. Black and red lines indicate the $(\sqrt{3} \times \sqrt{3})$ and (1×1) Brillouin zones of silicene. (f) and (g) Calculated band structures for silicene and Si_5Ge along the path indicated in (e). The contribution of the on-top, bridge, and hollow site atoms are respectively red, green, and blue colored in agreement with (d). The size of the circles represents the spectral weight of the combined contribution of Si and Ge atoms.

$E_{VBM}(x) - [E_{VBM}^{\text{silicene}}x + E_{VBM}^{\text{Si}_5\text{Ge}}(1-x)]$ with $bx(1-x)$ gives a bowing parameter b of -125 meV [see inset of Fig. 3(e)]. The absence of change in the line shape of the Zr $3d$ core-level photoelectron spectra upon deposition of germanium (Fig. 3 of the Supplemental Material [37]) indicates that there is no shift of the binding energy of the surface component. Therefore, the shift of the VBM cannot be explained by a variation of the surface dipole.

As shown in Figs. 4(a) and 4(b), the difference in band structure between silicene and Si_5Ge observed experimentally is well reproduced by DFT calculations. The band structures were calculated for structures with a lattice parameter artificially increased by 5% [11] to compensate the overestimation of the bandwidth caused by the generalized gradient approximation [39,40]. In agreement with the experimental ARPES spectra, the VBM is shifted upwards by 90 meV (from 200 to 110 meV), whereas the bottom of the band remains at the same energy (the width of the calculated band gap decreases from 290 to 200 meV).

To evaluate the influence of the epitaxial strain on the band structure of the $\text{Si}_{6-x}\text{Ge}_x$ alloy, the energy of the freestanding planarlike structures of silicene and Si_5Ge were calculated as a function of the lattice parameter of the unreconstructed silicene structure. To preserve the planarlike structure upon geometrical optimization in the absence of the substrate, the five Si atoms of the bottom layers were forced to remain in the same plane. In contrast to the slight increase of the equilibrium lattice parameter found for freestanding 2D hexagonal SiGe alloy [21], the planarlike structures of silicene and Si_5Ge have the same equilibrium lattice parameter of 3.89 \AA [Fig. 4(c)], corresponding to a compressive strain of 6.2%, which suggests that any strain-induced effect on the evolution of the band structure is negligible.

The good agreement between experimental and computed band structures allows for analyzing further the nature of the effect of the Ge atoms. Figures 4(f) and 4(g) show the respective contributions of on-top, hollow, and bridge site atoms, as indicated in Fig. 4(d), to the band structures of epitaxial sil-

icene and Si_5Ge plotted along the path indicated in Fig. 4(e). Please note that the calculations show some hybridization between the silicene (or Si_5Ge) states with the surface bands of ZrB_2 crossing the Fermi level. For both structures, the valence band centered on the K point appears to originate from the Si atoms in the bridge sites, whereas the conduction band minimum (CBM) centered on the M point of the Brillouin zone of the unreconstructed silicene originates from the Si atoms of the hollow sites. One can observe that in contrast to E_{VBM} , E_{CBM} the energy of the CBM does not vary much between the two structures. The comparison of the computed Mulliken charges carried by the different atoms (Table I) suggests that the on-top site Ge atoms are electron richer than the Si atoms in the same position, in agreement with the higher electronegativity of Ge (2.01) in comparison to that of Si (1.90). This induces an increase of the electron donation from the bridge site atoms, which are the first neighbors of the on-top site atoms and thus become further positively charged. In contrast, the charge carried by the hollow-site atoms does not vary significantly. This selective charge transfer from on-top site atoms to bridge site atoms results in a progressive shift of E_{VBM} towards the Fermi level, whereas E_{CBM} is fixed.

In conclusion, we experimentally demonstrated the possibility of fabricating an epitaxial silicene-like Si_5Ge compound by depositing a minute amount of Ge on silicene on $\text{ZrB}_2(0001)$ thin films on Si(111). For Ge coverages below $1/6$ ML, the deposition gives rise to a $\text{Si}_{6-x}\text{Ge}_x$ alloy based on the planarlike structure of epitaxial silicene in which the protruding sites are randomly occupied by Si or Ge atoms. The substitution of Si atoms by Ge atoms induces a shift of

TABLE I. Mulliken charges expressed in the number of e^- calculated by DFT.

	On-top	Bridge	Hollow
Silicene	-0.052	0.083	-0.016
Si_5Ge	-0.711	0.322	-0.020

the VBM, which suggests that it is possible to finely tune the band gap of the epitaxial $\text{Si}_{6-x}\text{Ge}_x$ by controlling the amount of Ge atoms.

We are thankful to Dr. Hiroyuki Yamane (IMS) for his assistance at beamline BL6U of UVSOR-III. A part of this work was supported by the Joint Studies Program of the Institute for Molecular Science Projects No. 203 (2016-

2017) and No. 206 (2017-2018). A.F. acknowledges financial support from JSPS KAKENHI Grant No. JP26790005. F.B.W. acknowledges financial support from the Foundation for Fundamental Research on Matter (FOM; Project No. 12PR3054), which is part of the Netherlands Organization for Scientific Research (NWO). Y.Y.-T. acknowledges financial support from Iketani Science and Technology Foundation.

-
- [1] C.-Z. Ning, L. Dou, and P. Yang, *Nat. Rev. Mater.* **2**, 17070 (2017).
- [2] L. Ci, L. Song, C. Jin, D. Jariwala, D. Wu, Y. Li, A. Srivastava, Z. F. Wang, K. Storr, L. Balicas, F. Liu, and P. M. Ajayan, *Nature Mater.* **9**, 430 (2010).
- [3] H.-P. Komsa and A. V. Krasheninnikov, *J. Phys. Chem. Lett.* **3**, 3652 (2012).
- [4] S.-H. Su, Y.-T. Hsu, Y.-H. Chang, M.-H. Chiu, C.-L. Hsu, W.-T. Hsu, W.-H. Chang, J.-H. He, and L.-J. Li, *Small* **10**, 2589 (2014).
- [5] Q. Fu, L. Yang, W. Wang, A. Han, J. Huang, P. Du, Z. Fan, J. Zhang, and B. Xiang, *Adv. Mater.* **27**, 4732 (2015).
- [6] K.-A. N. Duerloo and E. J. Reed, *ACS Nano* **10**, 289 (2016).
- [7] S. Susarla, A. Kutana, J. A. Hachtel, V. Kochat, A. Apte, R. Vajtai, J. C. Idrobo, B. I. Yakobson, C. S. Tiwary, and P. M. Ajayan, *Adv. Mater.* **29**, 1702457 (2017).
- [8] L. Tao, E. Cinquanta, D. Chiappe, C. Grazianetti, M. Fanciulli, M. Dubey, A. Molle, and D. Akinwande, *Nat. Nanotechnol.* **10**, 227 (2015).
- [9] K. Takeda and K. Shiraishi, *Phys. Rev. B* **50**, 14916 (1994).
- [10] S. Cahangirov, M. Topsakal, E. Aktürk, H. Şahin, and S. Ciraci, *Phys. Rev. Lett.* **102**, 236804 (2009).
- [11] C.-C. Lee, A. Fleurence, Y. Yamada-Takamura, T. Ozaki, and R. Friedlein, *Phys. Rev. B* **90**, 075422 (2014).
- [12] P. Vogt, P. De Padova, C. Quaresima, J. Avila, E. Frantzeskakis, M. C. Asensio, A. Resta, B. Ealet, and G. Le Lay, *Phys. Rev. Lett.* **108**, 155501 (2012).
- [13] Y. Feng, D. Liu, B. Feng, X. Liu, L. Zhao, Z. Xie, Y. Liu, A. Liang, C. Hu, Y. Hu *et al.*, *Proc. Natl. Acad. Sci. USA* **113**, 14656 (2016).
- [14] R. Quhe, Y. Yuan, J. Zheng, Y. Wang, Z. Ni, J. Shi, D. Yu, J. Yang, and J. Lu, *Sci. Rep.* **4**, 5476 (2014).
- [15] H. Şahin and F. M. Peeters, *Phys. Rev. B* **87**, 085423 (2013).
- [16] R. Friedlein, A. Fleurence, J. T. Sadowski, and Y. Yamada-Takamura, *Appl. Phys. Lett.* **102**, 221603 (2013).
- [17] M. Houssa, E. Scalise, K. Sankaran, G. Pourtois, V. V. Afanas'ev, and A. Stesmans, *Appl. Phys. Lett.* **98**, 223107 (2011).
- [18] T. H. Osborn, A. A. Farajian, O. V. Pupyseva, R. S. Aga, and L. C. Lew Yan Voon, *Chem. Phys. Lett.* **511**, 101 (2011).
- [19] B. Huang, H. J. Xiang, and S.-H. Wei, *Phys. Rev. Lett.* **111**, 145502 (2013).
- [20] H. Şahin, S. Cahangirov, M. Topsakal, E. Bekaroglu, E. Akturk, R. T. Senger, and S. Ciraci, *Phys. Rev. B* **80**, 155453 (2009).
- [21] J. E. Padilha, L. Seixas, R. B. Pontes, A. J. R. da Silva, and A. Fazzio, *Phys. Rev. B* **88**, 201106(R) (2013).
- [22] R.-W. Zhang, C.-W. Zhang, S.-S. Li, W.-X. Ji, P.-J. Wang, F. Li, P. Li, M.-J. Ren, and M. Yuan, *Solid State Commun.* **191**, 49 (2014).
- [23] A. Fleurence, Y. Yoshida, C.-C. Lee, T. Ozaki, Y. Yamada-Takamura, and Y. Hasegawa, *Appl. Phys. Lett.* **104**, 021605 (2014).
- [24] A. Fleurence, R. Friedlein, T. Ozaki, H. Kawai, Y. Wang, and Y. Yamada-Takamura, *Phys. Rev. Lett.* **108**, 245501 (2012).
- [25] Y. Yamada-Takamura, F. Bussolotti, A. Fleurence, S. Bera, and R. Friedlein, *Appl. Phys. Lett.* **97**, 073109 (2010).
- [26] W. Kohn and L. J. Sham, *Phys. Rev.* **140**, A1133 (1965).
- [27] J. P. Perdew, K. Burke, and M. Ernzerhof, *Phys. Rev. Lett.* **77**, 3865 (1996).
- [28] T. Ozaki, *Phys. Rev. B* **67**, 155108 (2003).
- [29] C.-C. Lee, Y. Yamada-Takamura, and T. Ozaki, *J. Phys.: Condens. Matter* **25**, 345501 (2013).
- [30] C.-C. Lee, A. Fleurence, R. Friedlein, Y. Yamada-Takamura, and T. Ozaki, *Phys. Rev. B* **88**, 165404 (2013).
- [31] L. Chen, C.-C. Liu, B. Feng, X. He, P. Cheng, Z. Ding, S. Meng, Y. Yao, and K. Wu, *Phys. Rev. Lett.* **109**, 056804 (2012).
- [32] L. Meng, Y. Wang, L. Zhang, S. Du, R. Wu, L. Li, Y. Zhang, G. Li, H. Zhou, W. A. Hofer, and H.-J. Gao, *Nano Lett.* **13**, 685 (2013).
- [33] T. Aizawa, S. Suehara, and S. Otani, *J. Phys. Chem. C* **118**, 23049 (2014).
- [34] M. Nogami, A. Fleurence, Y. Yamada-Takamura, and M. Tomitori, *Adv. Mater. Interfaces* **6**, 1801278 (2019).
- [35] A. Fleurence, T. G. Gill, R. Friedlein, J. T. Sadowski, K. Aoyagi, M. Copel, R. M. Tromp, C. F. Hirjibehedin, and Y. Yamada-Takamura, *Appl. Phys. Lett.* **108**, 151902 (2016).
- [36] T. G. Gill, A. Fleurence, B. Warner, H. Prüser, R. Friedlein, J. T. Sadowski, C. F. Hirjibehedin, and Y. Yamada-Takamura, *2D Mater.* **4**, 021015 (2017).
- [37] See Supplemental Material at <http://link.aps.org/supplemental/10.1103/PhysRevMaterials.5.L011001> for (1): the Ge site-dependence of the Si_5Ge structure energy determined by DFT, (2): Simulated STM images of $\text{Si}_{4.75}\text{Ge}_{0.25}$ structures and (3): Zr_{3d} core-level photoelectron spectra for different Ge coverages.
- [38] J. C. Aubry, T. Tylliszczak, A. P. Hitchcock, J.-M. Baribeau, and T. E. Jackman, *Phys. Rev. B* **59**, 12872 (1999).
- [39] D. E. Eastman, F. J. Himpsel, and J. A. Knapp, *Phys. Rev. Lett.* **44**, 95 (1980).
- [40] P. Haas, F. Tran, and P. Blaha, *Phys. Rev. B* **79**, 085104 (2009).